Identifying the Late Systolic Shoulder and its Determinants

James Cushway [*,**] **J. Geoffrey Chase** [*] **Thomas Desaive** [**] **Liam Murphy** [*]

[*] *University of Canterbury, Christ Church, New Zealand (e-mail: james.cushway@pg.canterbury.ac.nz).*
[**] *University of Liège (ULg), GIGA-in silico medicine, Liège, Belgium (e-mail: tdesaive@uliege.be)*

Abstract: The late systolic shoulder is an important point in the cardiac cycle. It is caused by the interaction between the forward and reflected waves within the arterial system. Important cardiovascular metrics, such as augmentation index, are calculated using the late shoulder. Furthermore, it is also used as an important input to many cardiovascular models. However, despite its importance, its definition throughout cardiovascular literature remains inconsistent. The late systolic shoulder is often observed as a late peak during systole, and this is widely accepted as its general definition. However, there is often no visible second peak, and identifying the late shoulder using this definition is not always possible. The shape of an arterial pressure wave is heavily dependant on the timing, magnitude and shape of both the forward and reflected waves. The patient specific nature of the late shoulder thus requires a patient specific approach for identification. Currently, there is no consensus algorithm which can reliably and accurately identify it. A few general algorithms have been proposed and accepted by the literature, however, they are known to provide inaccurate and inconsistent results. Given its clinical importance, a clearer definition of the late shoulder is required, and a reliable method for identification needs to be developed. This work aims to evaluate the currently used algorithms for identifying the late shoulder. Furthermore, waveform decomposition of the aortic pressure and flow wave is used to explore the relationship between the late shoulder and the forward and reflected waves, in an attempt to better understand the determinants of the late shoulder.

Keywords: Late systolic shoulder, aortic pressure, cardiovascular system

1. INTRODUCTION

The late systolic shoulder (SBP_2) is an important point in the cardiac cycle. It is used to define augmentation index (AIx), which is a key indicator of arterial stiffness and left ventricular afterload (Kelly et al. (1989); Nürnberger et al. (2002); Nichols et al. (2002); Takazawa et al. (2012); O'Rourke and Pauca (2004)). AIx has multiple definitions, but is most often defined as either the ratio of SBP_2 to the early systolic shoulder (Takazawa et al. (2012)), or as the ratio of the difference of SBP_2 and the early systolic shoulder, and the pulse pressure, giving AIx as a percentage of pulse pressure (Kelly et al. (1989)).

SBP_2 and pulse augmentation are caused by wave reflections in the arterial system. Wave reflections are generated at any impedance mismatch site in the arterial system including arterial bifurcations, blood vessel tapering and the high resistant peripheral vascular bed. These reflections interfere with forward travelling waves, causing constructive interference in pressure waves, and destructive interference in flow waves. The timing of this interference determines the magnitude of SBP_2 and AIx. In healthy, young individuals, the reflected wave tends to arrive later in the cardiac cycle, which results in a smaller SBP_2, causing a smaller AIx. However, in patients with stiffer arteries, such as elderly patients, waves travel faster, and the reflected wave intercepts the forward wave earlier in the cycle. This results in a larger SBP_2 and AIx.

Furthermore, SBP_2 is also an important input for cardiovascular modelling, specifically in the use of arterial transfer functions. Arterial transfer functions are used to recreate aortic pressure from peripheral pressure waveforms, since aortic pressure is not usually clinically available due to its highly invasive nature. SBP_2 is often used as an important input in the objective function of such transfer functions (Murphy and Chase (2023)). Aortic pressure is a key indicator of overall cardiovascular health (Takazawa et al. (2007); McEniery et al. (2014)), as well as a crucial input to cardiovascular models used for identifying important cardiovascular parameters (Cushway et al. (2022); Murphy et al. (2020); Murphy and Chase (2023); Pironet et al. (2015)). SBP_2 is thus potentially a crucial point for reliable identification of important cardiovascular parameters.

Despite its clinical importance and usefulness, SBP_2 is not very clearly defined. SBP_2 is generally taken to mean

⋆ This work was supported by EU H2020 ERA Permed JTC2021, "Personalised perfusion guided fluid therapy" and the EU H2020 R&I programme (MSCA-RISE-2019 call) under grant agreement #872488 — DCPM.

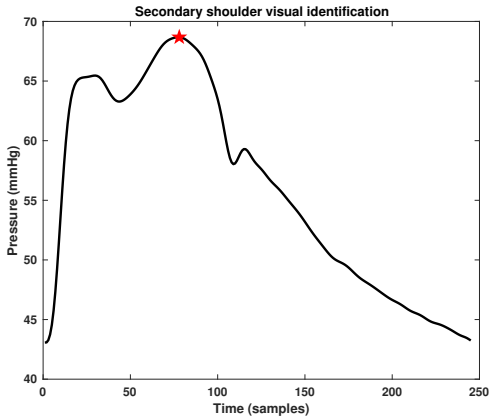

Fig. 1. Visual identification of SBP_2. SBP_2 can be visually identified as the second peak occurring during systole, marked by the red star.

the late peak in the aortic pressure, as shown in 1. In some cases, there are 2 obvious peaks, making SBP_2 easy to identify, both visually and mathematically. However, in many cases, the peaks are far less obvious, and are often indistinguishable, both visually and by mathematical methods, as depicted in Figure 2. SBP_2 is also a highly patient specific point, and identifying it by mathematical means is highly challenging.

Takazawa et al. (1995) posed a method for identifying SBP_2 using the fourth derivative of aortic pressure, which has since been widely adopted in the literature Nichols et al. (2022). However, this method is a generalisation, and several cases of erroneous results have been reported. Gatzka et al. (2001a,b); Söderström et al. (2002) all reported AIx measures of over 50%, which should not be possible (Nichols et al. (2022)). There are also devices available which use proprietary algorithms for locating $pSBP_2$, such as SphygmoCor. However, even with these clinically approved devices, studies have encountered cases where $pSBP_2$ was indeterminable Zhang et al. (2011).

This study uses data from pig experiments performed at the University of Liège in Belgium to evaluate previous algorithms posed for identifying SBP_2, as well as separating invasive aortic blood pressure measurements waves into their constituent components to identify the determinants of SBP_2 and provide a clearer understanding of what exactly SBP_2 is.

2. METHODS

2.1 Experimental Procedure

The experimental protocol was approved by the Ethics Committee for the use of animals at the University of Liege, Belgium between September - November, 2015 (Reference Number 14–1726). Five pure Pietrain pigs were anaesthetised and mechanically ventilated. Septic shock was then induced in the subjects via a single infusion of endotoxin (lipopolysaccharide from E. Coli, 0.5 mg/kg, infused over 30 min). Pre-endotoxin infusion, a 500 mL saline solution was administered over 30 min simulating fluid resuscitation therapy. Aortic pressure in the subjects was continually measured via a catheter with a sampling

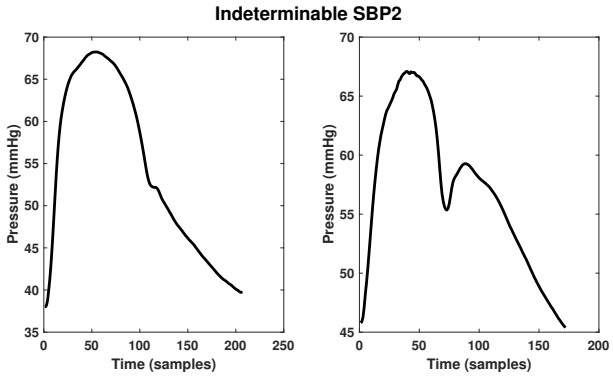

Fig. 2. Aortic pressure waves displaying different types of indeterminable SBP_2 points. The first wave has a reflected wave which arrives very early in systole, and the second wave has very late arriving reflected wave.

rate of 250 Hz. Left ventricle pressure and volume were also continually measured at 250 Hz via an admittance pressure volume catheter inserted into the left ventricle via an apical stab.

2.2 Waveform Decomposition

The aortic pressure wave can be decomposed into its forward and reflected waves using the reflection coefficient:

$$\Gamma = \frac{Z_{in} - Z_c}{Z_{in} + Z_c} \tag{1}$$

$$P_f = \frac{P_{ao}}{1 + \Gamma} \tag{2}$$

$$P_b = \Gamma P_f \tag{3}$$

where P_{ao}, P_f, and P_b are the aortic, forward and reflected pressure waves respectively, Γ is the reflection coefficient, and Z_{in} and Z_c are the input and characteristic impedance of the aorta respectively. Input impedance can be found using the fourier series approximations of aortic pressure and flow:

$$Z_{in}(j\omega) = \frac{P_{ao}(j\omega)}{Q_{ao}(j\omega)} \tag{4}$$

where $Z_{in}(j\omega)$ is the input impedance Fourier series, $P_{ao}(j\omega)$ is the aortic pressure Fourier series and $Q_{ao}(j\omega)$ is the aortic flow Fourier series. Matlab's fft algorithm was used to transform aortic pressure and flow into their Fourier series equivalents.

Characteristic impedance can be approximated by taking the mean of the upper harmonics of input impedance. Varying harmonic intervals have been used throughout the literature. This work chose to use harmonics 4 - 10, which was in line with other works (Hughes AD (2009); Tabima et al. (2012)).

The characteristic and input impedance were used to calculate the reflection coefficient using Eq. 1. Thereafter, the forward and reflected waves were calculated using Eq. 2 and Eq. 3 respectively. The forward and reflected waves were then converted back into the time domain using Matlabs ifft algorithm.

2.3 Determining of SBP_2

Takazawa et al. (1995) used the fourth derivative of the aortic pressure wave with respect to time (d^4P_{ao}) is used to determine SBP_2. If the gradient of d^4P_{ao} corresponding to aortic peak pressure is positive, this point is used as SBP_2. If the slope of d^4P_{ao} corresponding to peak aortic pressure is negative, the third zero crossing from below to above is used to determine SBP_2.

2.4 Analyses

Once all forward and reflected waves and SBP_2 points were calculated, forward and reflected waves were verified by matching the peak of the forward wave to the peak of aortic flow, since the peak of the forward wave should coincide with the peak of flow O'Rourke and Pauca (2004). The SBP_2 points were verified by visually identifying SBP_2 in 100 beats per pig and comparing it to computed SBP_2 values. Beats were chosen if they showed a prominent secondary peak which could be easily visually identified. An example of a visually identified SBP_2 is shown in Figure 1. The percentage of correctly identified points was recorded, and for incorrectly calculated points, the average error (in samples) between the correct and incorrect points was recorded.

To better understand SBP_2, and any potential determinants, the relationship between SBP_2 and the forward and reflected waves was examined, specifically looking at the shapes of the forward and reflected waves compared to the location of SBP_2.

3. RESULTS

3.1 Waveform Decomposition

Waveform decomposition was verified by ensuring the peaks of the forward pressure wave and the aortic flow wave matched. From the 4 pigs, a total of 8691 beats were decomposed. The error between the forward wave peak and peak flow was calculated as a percentage of the total beat length. The overall error across all beats for all pigs was $4.29 \pm 2.87\%$. The error for each pig is shown in Table 1. It should be noted that flow waveforms are very noisy, and noise present may cause a slight shift in perceived peaks, which causes peak values to slightly vary from beat to beat. Despite this, the small errors show the peaks of flow and forward waves align, demonstrating the forward wave has been correctly identified. A decomposition from each pig is shown in Figure 3.

Table 1. Flow and forward wave peak errors

Pig	Error (%)
1	4.93 ± 2.14
2	2.39 ± 1.81
3	5.81 ± 3.23
4	3.92 ± 1.55

3.2 SBP_2

SBP_2 was calculated using the method proposed by Takazawa et al. (1995). The location of SBP_2 was verified by means of visual inspection, by inspecting 100 beats from each pig. The location of the secondary shoulder was taken as any visible late systolic peak. The secondary shoulder was deemed to have been correctly identified if it fell within a 10 sample window of the visually identified SBP_2. The percentage of correctly identified secondary systolic shoulder points is shown in table 2. For incorrect beats, the average error (in samples) is also recorded in table 2. Examples of a correct and incorrect identification of SBP_2 for each pig is shown in 4. Pig's 3 and 4 displayed a 0% success. This was because the peak of the aortic pressure wave always coincided with the primary shoulder, and the third zero crossing from above to below of the 4th derivative always occurred before this peak. The algorithm was thus not capable of finding SBP_2 for these pigs.

Table 2. Secondary shoulder errors.

Pig	Correctly identified (%)	Error(samples)
1	58	38.09 ± 18.57
2	71	51.37 ± 3.17
3	0	54.32 ± 6.79
4	0	51.42 ± 3.70

3.3 SBP_2 and the forward and reflected wave

The reflected wave was plotted alongside the aortic pressure and SBP_2 to gain further insight into the relationship between SBP_2 and the reflected wave. Figure 5 shows a reflected and aortic waves and SBP_2 for each pig. Unsurprisingly, SBP_2 occurs near the peak of the reflected wave, and the inflection point occurring in the aortic pressure wave preceding SBP_2 can be seen to occur just after the foot of the reflected wave. The same 100 beats were analysed, and the distance between the visually identified SBP_2 and the peak of the reflected wave was recorded. The gap between the peak of the reflected wave and SBP_2 remained relatively constant, and the results are shown in table 3.

Table 3. Distance between reflected wave peak and SBP_2

Pig	Distance (samples)
1	30.42 ± 2.47
2	22.45 ± 5.46
3	23.8 ± 5.46
4	22.18 ± 1.01

Figure 6 shows $SBP2$ plotted on top of the forward wave. As can be seen from the figure, the forward may also possesses a shoulder where SBP_2 is located. This shows the exact location of SBP_2 is not only dependent on the timing of the reflected wave, but also on the shape of the forward travelling wave.

4. DISCUSSION

4.1 Calculated SBP_2

The proposed method from Takazawa et al. (1995) did not perform well on this data. For 2 of the pigs, it could not correctly identify SBP_2 in any beats. The other 2 pigs showed a 58% and 71% success rate. This result is indicative of the highly variable nature of the secondary

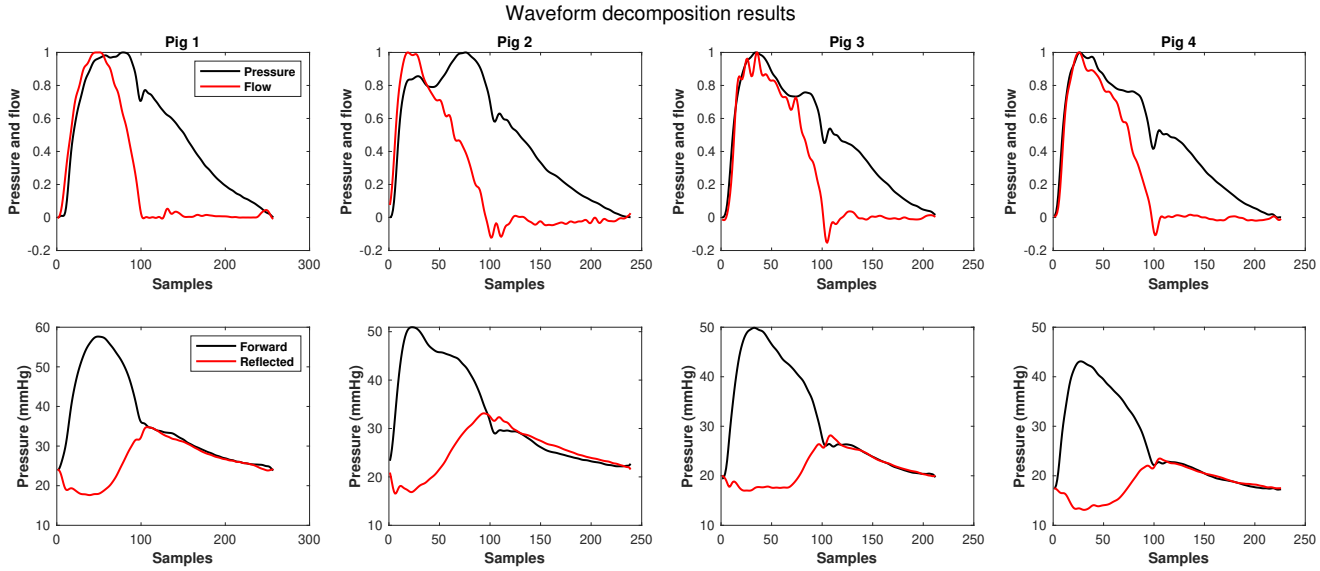

Fig. 3. Pressure decomposition of a beat from each pig. The top row shows the aortic flow and pressure wave for each pig, normalised to a peak flow and pressure of 1, and the lower row shows the corresponding decomposed forward and reflected pressure waves.

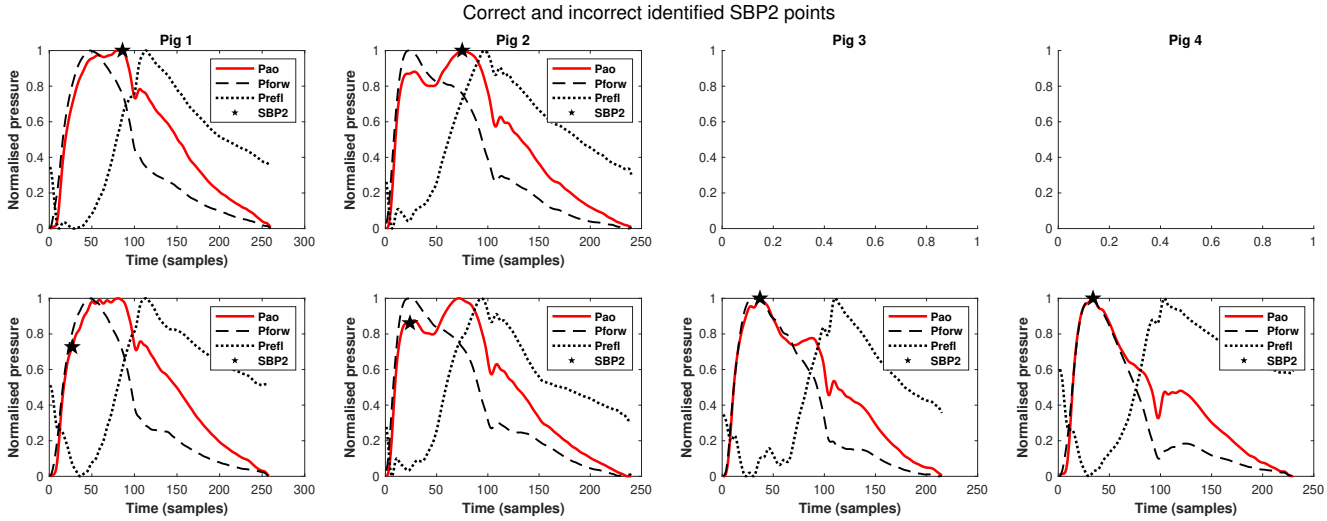

Fig. 4. Identified SBP_2 for all pigs. The upper row of plots represent correctly located points, while the lower row represents incorrectly located points. Aortic pressure, the forward wave, and the reflected wave are represented by the red, black dashed and black dotted lines respectively. SBP_2 is represented by the star. Note Pig's 3 and 4 had no correctly identified $SBP2$ points.

systolic shoulder and a simple count of fourth derivative features is insufficient to identify it.

The poor performance of the algorithm is due to several factors. Firstly, while it is likely the algorithm developed by Takazawa et al. (1995) best suited their data and provided good results, it is a generalisation, and does not adapt well to other data. Furthermore, even if the method was patient specific, it uses 4th derivatives for the identification of SBP_2 and is thus highly susceptible to noise. Even small amounts of noise in the original waveform can result in large oscillations in the 4th derivative. The data used in this study is considered to be much higher fidelity than data from bedside machines. However, the noise present still posed a large problem, and rendered the zero crossing method highly inaccurate. It is possible to heavily filter the original waveform. However, heavy filtering causes loss of information from the waveform, and important features in the 4th derivative may be lost, which may also yield incorrect results.

4.2 SBP_2 and the forward and reflected waves

The above-mentioned flaws of the algorithm are not the only problems when attempting to identify SBP_2. It is also the blurry definition of SBP_2 itself. Usually, SBP_2 is taken to mean the late peak in systole caused by wave reflections. However, there is often no distinguishable second peak.

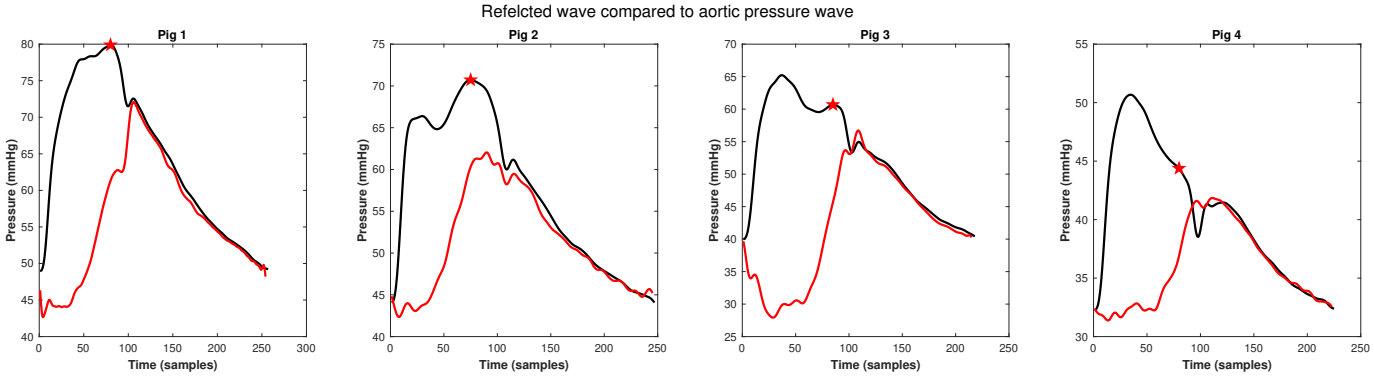

Fig. 5. Reflected wave compared to aortic pressure wave and SBP_2. The reflected wave is plotted in red, the aortic wave in black and SBP_2 is the red star. The magnitude of the reflected wave has been doubled for better visual comparison.

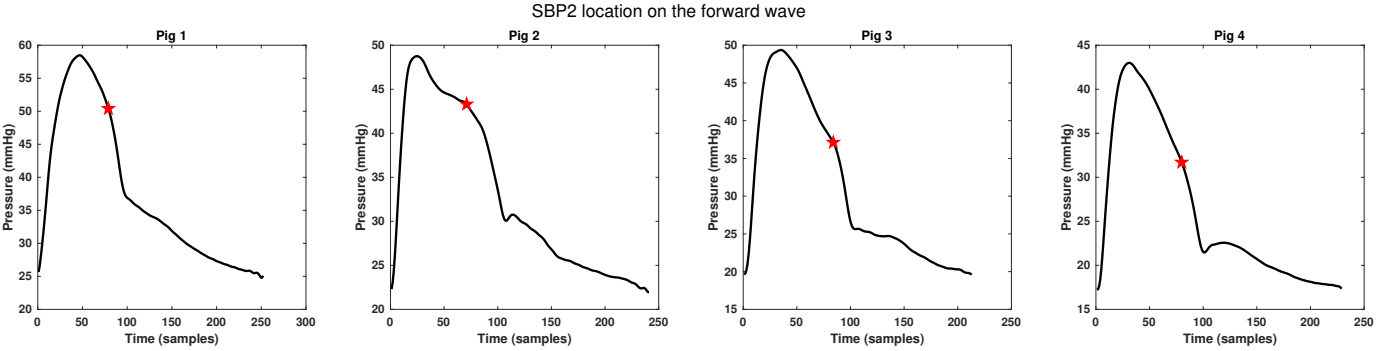

Fig. 6. SBP_2 plotted on the forward wave for all pigs. The forward wave is plotted in black and SBP_2 is represented by the red star.

Indeed, as shown in figure 2, SBP_2 is indistinguishable. SBP_2 is largely dependent on 3 major factors: timing, magnitude, and shape of the reflected wave. Figure 2 depicts 2 cases: 1) the reflected wave arrives early enough in systole for it to create one large peak, where neither the early or late shoulders are identifiable, and 2) the reflected wave arrives late enough for there to be little to no visible effect in systole and SBP_2 is not determinable. It is therefore insufficient to design an algorithm which just searches for a second peak or inflection point during systole.

A more appropriate definition of the secondary shoulder would be the point of maximum interaction between the forward and reflected wave. This usually occurs close to the peak of the reflected wave. However, it also occurs very near to the shoulder of the forward wave, showing SBP_2 is also dependent on the shape of the forward wave. On some forward travelling waves, there is a clear shoulder in late systole. The shoulder on the forward wave could be caused by late atrial ejection during systole. It could also be due to a reflected wave which has reached the terminal of the aorta and has been re-reflected, becoming a forward travelling wave. Since this waveform decomposition can only decompose the aortic waveform into a net forward and net reflected wave, it is not possible to tell if this could be the cause.

Important timing locations on the reflected wave, such as the foot and peak, and any potential identifiable shoulders on the forward wave may assist in locating SBP_2. However, in a clinical setting, there is no access to the flow wave, and waveform decomposition would not be possible. Westerhof et al. (2006) performed waveform decomposition using aortic pressure alone. Since only peripheral arterial pressure is available in an ICU setting, this could be performed on peripheral arteries as well. However, the flow waveform in peripheral arteries is more complex than aortic flow, and, to the authors knowledge, there is little to no information on simple modelling of a peripheral flow waveform in the literature. The inverse relationship may also apply between SBP_2 and the reflected waves. SBP_2 gives important timing information as to the whereabouts of the reflected wave, and may be used to estimate reflected wave timings in absence of a flow waveform.

5. CONCLUSION

This work investigated an established method for determining SBP_2, as well as investigating the determinants of SBP_2 and its relationship with the forward and backward waves. Ultimately, the method posed by Takazawa et al. (1995) for finding SBP_2 did not perform well, and was unable to locate SBP_2 in any beats for 2 of the 4 pigs. The poor performance of this algorithm is likely due to the fact this algorithm relies on the fourth derivative of pressure, which is highly sensitive to noise. However, the method is also a generalisation, and while it may have fitted the original data set well, it does not appear to adapt well to other data. Given the patient specificity of SBP_2, it seems

clear any generalised algorithm used for identifying SBP_2 would likely be susceptible to similar issues, and any works using such algorithms should apply caution in doing so.

SBP_2 functions as an important point for determining clinical metric such as AIx, as well as a model input for identifying central pressure from peripheral pressures. Being able to accurately identify it could prove crucial for cardiovascular assessment as well as model based clinical care. Given the patient specific nature of SBP_2, a patient specific algorithm is required to accurately and reliably identify it. Waveform decomposition is a simple method which can be used to assist identifying in SBP_2. Currently, given flow waveforms are not usually available clinically, waveform decomposition may not be possible in a clinical setting. However, as shown by Westerhof et al. (2006), this could be overcome by simple modelling of the flow waveform.

ACKNOWLEDGEMENTS

This work was supported by EU H2020 ERA Permed JTC2021, "Personalised perfusion guided fluid therapy".

The project was supported by EU H2020 R&I programme (MSCA-RISE-2019 call) under grant agreement #872488 — DCPM.

REFERENCES

Cushway, J., Murphy, L., Chase, J.G., Shaw, G.M., and Desaive, T. (2022). Physiological trend analysis of a novel cardio-pulmonary model during a preload reduction manoeuvre. *Computer Methods and Programs in Biomedicine*, 220, 106819. doi: https://doi.org/10.1016/j.cmpb.2022.106819.

Gatzka, C.D., Cameron, J.D., Dart, A.M., Berry, K.L., Kingwell, B.A., Dewar, E.M., Reid, C.M., and Jennings, Garry L.R., f.t.A.I. (2001a). Correction of carotid augmentation index for heart rate in elderly essential hypertensives. *American Journal of Hypertension*, 14(6), 573–577. doi:10.1016/S0895-7061(00)01320-0.

Gatzka, C.D., Kingwell, B.A., Cameron, J.D., Berry, K.L., Liang, Y.L., Dewar, E.M., Reid, C.M., Jennings, G.L., Dart, A.M., and the ANBP2 investigators (2001b). Gender differences in the timing of arterial wave reflection beyond differences in body height. *Journal of Hypertension*, 19(12), 2197–2203. doi:10.1097/00004872-200112000-00013.

Hughes AD, P.K. (2009). Forward and backward waves in the arterial system: impedance or wave intensity analysis? *Med Biol Eng Comput.*, 47, 207–210. doi: 10.1007/s11517-009-0444-1.

Kelly, R., Hayward, C., Avolio, A., and O'Rourke, M. (1989). Noninvasive determination of age-related changes in the human arterial pulse. *Circulation*, 80(6), 1652–1659. doi:10.1161/01.CIR.80.6.1652.

McEniery, C.M., Cockcroft, J.R., Roman, M.J., Franklin, S.S., and Wilkinson, I.B. (2014). Central blood pressure: current evidence and clinical importance. *European Heart Journal*, 35(26), 1719–1725. doi: 10.1093/eurheartj/eht565.

Murphy, L. and Chase, J.G. (2023). Single measurement estimation of central blood pressure using an arterial transfer function. *Computer Methods and Programs in Biomedicine*, 229, 107254. doi: https://doi.org/10.1016/j.cmpb.2022.107254.

Murphy, L., Davidson, S., Chase, J.G., Knopp, J.L., Zhou, T., and Desaive, T. (2020). Patient-specific monitoring and trend analysis of model-based markers of fluid responsiveness in sepsis: A proof-of-concept animal study. *Ann Biomed Eng*, 48, 682–694. doi: https://doi.org/10.1007/s10439-019-02389-9.

Nichols, W., Singh, A., and Balkrishna, M. (2002). Augmentation index as a measure of peripheral vascular disease state. *Current Opinion in Cardiology*, 17.

Nichols, W.W., O'Rourke, M., Edelman, E.R., and Vlachopoulos, C. (2022). *McDonald's blood flow in arteries.* CRC Press, 7 edition.

Nürnberger, J., Keflioglu-Scheiber, A., Saez, A.O., Wenzel, R., Philipp, T., and Schäfers, R. (2002). Augmentation index is associated with cardiovascular risk. *Journal of Hypertension*, 20(12), 2407–2414.

O'Rourke, M.F. and Pauca, A.L. (2004). Augmentation of the aortic and central arterial pressure waveform. *Blood Pressure Monitoring*, 9(4), 179–185.

Pironet, A. et al. (2015). Model-based stressed blood volume is an index of fluid responsiveness. *IFAC-PapersOnLine*, 48(20), 291–296. doi: https://doi.org/10.1016/j.ifacol.2015.10.154. 9th IFAC Symposium on Biological and Medical Systems BMS 2015.

Söderström, S., Nyberg, G., O'Rourke, M.F., Sellgren, J., and Pontén, J. (2002). Can a clinically useful aortic pressure wave be derived from a radial pressure wave? *BJA: British Journal of Anaesthesia*, 88(4), 481–488. doi:10.1093/bja/88.4.481.

Tabima, D.M., Roldan-Alzate, A., Wang, Z., Hacker, T.A., Molthen, R.C., and Chesler, N.C. (2012). Persistent vascular collagen accumulation alters hemodynamic recovery from chronic hypoxia. *Journal of Biomechanics*, 45(5), 799–804. doi: https://doi.org/10.1016/j.jbiomech.2011.11.020. Special Issue on Cardiovascular Solid Mechanics.

Takazawa, K., Tanaka, N., Takeda, K., Kurosu, F., and Ibukiyama, C. (1995). Underestimation of vasodilator effects of nitroglycerin by upper limb blood pressure. *Hypertension*, 26(3), 520–523. doi: 10.1161/01.HYP.26.3.520.

Takazawa, K. et al. (2007). Relationship between radial and central arterial pulse wave and evaluation of central aortic pressure using the radial arterial pulse wave. *Hypertension Research*, 30, 219–228. doi: 10.1291/hypres.30.219.

Takazawa, K. et al. (2012). Estimation of central aortic systolic pressure using late systolic inflection of radial artery pulse and its application to vasodilator therapy. *Journal of Hypertension*, 30(5), 908–916. doi: 10.1097/HJH.0b013e3283524910.

Westerhof, B.E., Guelen, I., Westerhof, N., Karemaker, J.M., and Avolio, A. (2006). Quantification of wave reflection in the human aorta from pressure alone. *Hypertension*, 48(4), 595–601. doi: 10.1161/01.HYP.0000238330.08894.17.

Zhang, Y. et al. (2011). Radial late-sbp as a surrogate for central sbp. *Journal of Hypertension*, 29(4), 676–681. doi:10.1097/HJH.0b013e328342f05f.